DALTON
FULL PAPER

Cyclic and open-chain aza–oxa ferrocene-functionalised derivatives as receptors for the selective electrochemical sensing of toxic heavy metal ions in aqueous environments

José M. Lloris,[a] Ramón Martínez-Máñez,*[a] Miguel E. Padilla-Tosta,[a] Teresa Pardo,[a] Juan Soto,[a] Paul D. Beer,*[b] James Cadman[b] and David K. Smith[b]

[a] *Departamento de Química, Universidad Politécnica de Valencia, Camino de Vera s/n, 46071 Valencia, Spain. E-mail: rmaez@qim.upv.es*
[b] *Inorganic Chemistry Laboratory, University of Oxford, South Parks Road, Oxford, UK OX1 3QR. E-mail: paul.beer@inorganic.chemistry.oxford.ac.uk*

Received 15th March 1999, Accepted 19th May 1999

A new family of aza–oxa open-chain and macrocyclic molecules functionalised with ferrocenyl groups have been synthesized and characterised. The crystal structures of the $[HL^1][PF_6]$, $[H_2L^3][PF_6]_2$, $[H_2L^4][PF_6]_2$ and $[H_2L^5][PF_6]_2$ salts have been determined by single crystal X-ray procedures {L^1 = 10-ferrocenylmethyl-1,4,7-trioxa-10-azacyclododecane, L^3 = 7,13-bis(ferrocenyl)-1,4,10-trioxa-7,13-diazacyclopentadecane, L^4 = 1,8-bis[bis(ferrocenylmethylamino)]-3,6-dioxaoctane, L^5 = 1,8-bis(ferrocenylmethylamino)-3,6-dioxaoctane}. They consist of cationic protonated amines linked *via* ionic interactions with hexafluorophosphate anions. Additionally hydrogen-bonding interactions have also been found. The receptors have been designed to promote discrimination, using electrochemical techniques, between toxic heavy metal ions such as Hg^{2+} over other commonly water present cations in aqueous environments. The presence in the receptors of oxygen and nitrogen donor atoms has been used to control the selectivity of large metal ions over small ones. Potentiometric and electrochemical studies have been mainly carried out to find pH ranges of selective electrochemical recognition. Potentiometric titrations were carried out in water (25 °C, 0.1 mol dm^{-3} potassium perchlorate) for L^1 and L^2 [1,1′-(5,8-dioxa-2,11-diazadodecane-1,12-diyl)-ferrocene] and in 1,4-dioxane–water (25 °C, 0.1 mol dm^{-3} potassium nitrate) for L^3 and L^5 with Ni^{2+}, Cu^{2+}, Zn^{2+}, Cd^{2+}, Pb^{2+} and Hg^{2+}. All receptors show larger stability constants with Hg^{2+} than with the remaining metal ions studied. This is especially so for L^1 and L^2. The receptors L^1, L^2 and L^5 are able electrochemically and selectively to sense the presence of Hg^{2+}, whereas maximum electrochemical shifts are produced in L^3 upon addition of Pb^{2+}. Of importance is the large and selective electrochemical shift monitored in water for L^2 and Hg^{2+} with an anodic displacement of the oxidation potential of *ca.* 130 mV which is one of the largest shifts ever reported in electrochemical cation sensing in water using related receptors. A good agreement has been found between potentiometric and electrochemical results. Selective electrochemical response against Hg^{2+} appears to be associated with (i) pH ranges of selective complexation or (ii) the existence of strong predominant receptor–metal complexes in a wide pH range. Additionally the electrochemical behaviour of receptors L^1 and L^2 in the presence of metal ions can be roughly predicted from potentiometric data. The stability constants of the complexes between L^1 and Cu^{2+}, Cd^{2+}, Pb^{2+} and Hg^{2+} were also determined in the presence of Cl^-. Whereas there is no important change in the stability constants of the L–H^+–M^{2+} systems when $M^{2+} = Cu^{2+}$, Cd^{2+} or Pb^{2+}, there is a decrease of the co-ordination ability of L^1 towards Hg^{2+}. This is also reflected in electrochemical studies which demonstrate that $[Hg(L^1)]^{2+}$ electrochemically sense Cl^- at pH 7. To the best of our knowledge this is the first time it has been shown that metal complexes functionalised with ferrocenyl groups can electrochemically sense anions.

Introduction

The development of new advances in supramolecular chemistry for the progress of new aspects that could be of use in sensing properties or sensor technologies is an area of recent interest. Among current advances in this area are molecules that are able to change an easily measurable physical property upon guest co-ordination. These molecules combine the presence of two components, (i) binding sites and (ii) molecular antennas, that could undergo a change in redox[1] or photo-physical[2] properties upon co-ordination of target species. A combination of well known properties and suitable redox-active groups has proved an adequate method strategically to design new receptors for the electrochemical sensing of substrates.[1] This strategy comprises the selection of an appropriate binding site with a prominent affinity for a target substrate and its functionalisation with ferrocenyl or other redox groups. Following this approximation many systems have been reported to be able electrochemically to sense the presence of anionic, cationic and neutral molecules. However most of these studies have been carried out in non-aqueous solvents. In aprotic solvents the number of possible species is usually limited. In contrast, the situation in aqueous environments can be quite complex, especially if both receptor and guest protonate in the pH range of study. However one can take advantage of the rich chemistry that is found in aqueous environments and the competition between proton and guest to select pH ranges of selective sensing.[3–25] Although the first reported receptor able to recognise the presence of metal ions in aqueous environments was a ferrocenophane containing N- and O-donor atoms,[3] most of the later studies were carried out on ferrocene-functionalised polyaza open-chain or cyclic derivatives. We are interested in amplifying these studies and demonstrate that using ferrocene-functionalised polyazaalkanes the selectivity against target metal ions could be modulated by controlling the nature of the donor atoms. For instance the incorporation of O-donor atoms, especially in macrocycles, can be used to control the selectivity for large metal ions over small ones. Thus the functionalisation with ferrocenyl groups of aza–oxa open chain or cyclic molecules could be an approach to developing sensing receptors for the electrochemical recognition of toxic heavy ions of environmental importance such as Hg^{2+}.

By means of incorporating the redox-active ferrocene moiety into aza–oxa ligand frameworks, we report a study of the potential sensing behaviour against large metal ions of a family of ferrocene-functionalised aza–oxa derivatives in water and 1,4-dioxane–water mixtures. The work has been mainly focused on finding pH ranges of selective electrochemical recognition.

Experimental

Physical measurements

Electrochemical data were obtained with a Tacussel IMT-1 programmable function generator, connected to a Tacussel PJT 120-1 potentiostat. The working electrode was graphite with a saturated calomel reference electrode separated from the test solution by a salt bridge containing the solvent/supporting electrolyte. The auxiliary electrode was platinum wire. Potentiometric titrations were carried out in water (0.1 mol dm^{-3} potassium perchlorate, 25 °C) for L^1, L^2 and in 1,4-dioxane–water (70:30 v/v, 0.1 mol dm^{-3} potassium nitrate, 25 °C) for L^3 and L^5 using a reaction vessel water-thermostatted at 25.0 ± 0.1 °C under nitrogen. The titrant was added by a Crison 2031 microburette. The potentiometric measurements were made using a Crison 2002 pH-meter and a combined glass electrode. A PC automatically controlled the titration system. The electrode was calibrated as a hydrogen concentration probe by titration of well known amounts of HCl with CO_2-free KOH solution and determining the equivalence point by Gran's method[26] which gives the standard potential E'° and the ionic product of water ($K'_w = [H^+][OH^-]$). The computer program SUPERQUAD[27] was used to calculate the protonation and stability constants. The titration curves for each system (*ca.* 250 experimental points corresponding to at least three titration curves, pH = −log[H], range investigated 2.5–10, concentration of the ligand and anions *ca.* 1.2×10^{-3} mol dm^{-3}) were treated either as a single set or as separated entities without significant variations in the values of the stability constants.

Preparations

L^1. The synthesis of receptor L^1 has been published elsewhere.[21] The compound 10-aza-12-crown-4 (250 mg, 1.43 mmol) and (ferrocenylmethyl)trimethylammonium iodide (550 mg, 1.43 mmol) were heated to reflux in dry acetonitrile (100 cm^3) for 24 h. The reaction mixture was filtered and the orange solution evaporated to dryness. The resulting oil was dissolved in dichloromethane and chromatographed using dichloromethane–methanol (100:0.5) as eluent. Yield 430 mg, 80% (Found: C, 57.47; H, 7.21; N, 3.61. $C_{18}H_{27}FeNO_3 \cdot H_2O$ requires C, 58.33; H, 7.41; N, 3.58%). NMR ($CDCl_3$): ^1H, δ 4.14, 4.08 (t, C_5H_4, 4 H), 4.09 (s, C_5H_5, 5 H), 3.67, 3.66, 3.56 (t, CH_2, 12 H), 3.57 (s, CH_2, 2 H) and 2.65 (t, CH_2, 4 H); ^{13}C-{^1H}, δ 82.81 (C_{ipso}, C_5H_4), 70.87, 70.26, 69.75 (CH_2), 70.06, 67.81 (C_5H_4), 68.30 (C_5H_5), 55.70, 53.79 (CH_2). Mass spectrum (FAB): 374 (M^+).

Compounds L^3 and L^4 were synthesized in a similar fashion.

L^2. Ferrocene-1,1′-dicarbaldehyde (0.26 g, 1.07 mmol) dissolved in 10 cm^3 of dry acetonitrile and 2,2′-(ethylenedioxy)-bis(ethylamine) (0.15 g, 1.01 mmol) also in 10 cm^3 of dry acetonitrile were added simultaneously to 30 cm^3 of dry acetonitrile with stirring under N_2 in darkness for 48 h. The solution was then filtered and the acetonitrile removed *in vacuo* leaving an orange oil. This oil was dissolved in 50 cm^3 methanol and small portions of $NaBH_4$ were added. The solution was stirred at room temperature for 3 h after which the methanol was removed and dichloromethane added. The suspension was filtered and the dichloromethane removed. The oil was dissolved in acetone and refluxed for 2 h and then filtered. The acetone was finally removed. The orange oil was purified by column chromatography on silica gel using 95:5, methanol–ammonium hydroxide. The product was collected in 50% yield as an orange oil. This was converted into its hydrochloride salt by bubbling HCl through a solution of the amine in dry diethyl ether. The salt was collected in quantitative yield by filtration (Found: C, 47.70; H, 7.05; N, 5.73. $C_{18}H_{28}FeN_2O_2 \cdot 2HCl \cdot H_2O$ requires C, 48.13; H, 6.73; N, 6.24%). NMR ($CDCl_3$): ^1H, δ 4.14, 4.10 (t, C_5H_4, 8 H), 3.67 (t, CH_2, 8 H), 3.57 (s, CH_2, 4 H) and 2.88 (t, CH_2, 4 H); ^{13}C-{^1H}, δ 88.07 (C_{ipso}, C_5H_4), 70.75 (CH_2), 70.08 (CH_2), 68.13 (C_5H_4), 67.54 (C_5H_4), 48.52 (CH_2) and 47.78 (CH_2).

L^3. The compounds 7,13-diaza-15-crown-5 (0.4 g, 1.83 mmol) and (ferrocenylmethyl)trimethylammonium iodide (2.12 g, 5.5 mmol) were heated in dry acetonitrile (150 cm^3). Purification was as above for L^1. Yield 923 mg, 82% (Found: C, 39.37; H, 4.95; N, 2.82. $C_{32}H_{42}Fe_2N_2O_3 \cdot 2HPF_6 \cdot CH_2Cl_2 \cdot H_2O$ requires C, 39.27; H, 4.80; N, 2.78%). NMR ($CDCl_3$): ^1H, δ 4.15, 4.09 (t, C_5H_4, 8 H), 4.10 (s, C_5H_5, 10 H), 3.59 (s, CH_2, 8 H) 3.54 (t, CH_2, 8 H), 2.70 (t, CH_2, 4 H) and 2.69 (t, CH_2, 4 H); ^{13}C-{^1H}, δ 82.38 (C_{ipso}, C_5H_4), 70.33 (CH_2), 70.15 (C_5H_4), 69.73, 68.94 (CH_2), 68.37 (C_5H_5), 67.91(C_5H_4), 55.38, 53.35 and 53.20 (CH_2). Mass spectrum (FAB): 637 (M + Na) and 614 (M^+).

L^4. From 2,2′-(ethylenedioxy)bis(ethylamine) (0.313 cm^3, 2.144 mmol) and (ferrocenylmethyl)trimethylammonium iodide (3.3 g, 8.57 mmol). Purification as above. Yield 1.23 g, 60% (Found: C, 62.33; H, 6.26; N, 2.93. $C_{50}H_{56}Fe_4N_2O_2 \cdot H_2O$ requires C, 62.68; H, 6.05; N, 2.92%). NMR ($CDCl_3$): ^1H, δ 4.18, 4.11 (t, C_5H_4, 16 H), 4.08 (s, C_5H_5, 20 H), 3.52 (s, CH_2, 4 H) 3.46 (t, CH_2, 4 H), 3.45 (s, CH_2, 8 H) and 2.54 (t, CH_2, 4 H); ^{13}C-{^1H}, δ 83.46 (C_{ipso}, C_5H_4), 70.22 (C_5H_4), 69.98 (CH_2), 68.48 (C_5H_5), 67.88 (C_5H_4), 53.42, 51.41 (CH_2). Mass spectrum (FAB): 941 (M^+).

L^5. This was synthesized following ref. 28.

Crystal structure determinations

X-Ray data were collected on a Siemens P4 four-circle diffractometer using monochromatised Mo-Kα radiation. Unit-cell dimensions were determined from the angular settings of 35 reflections. The intensity of three standard reflections monitored every 100 showed no systematic variations. Lorentz-polarisation corrections were applied. The structures were solved and refined by full-matrix least squares on F^2 using the computer program SHELXTL.[29] Table 1 shows the crystal data.

$[HL^1][PF_6]$. Crystals were obtained by slow diffusion of hexane into dichloromethane solutions of the $[HL^1][PF_6]$ salt. ψ-Scan absorption corrections were applied (maximum and minimum transmission 0.347 and 0.317). The structure was solved using direct methods. Anisotropic thermal parameters were used for all non-hydrogen atoms. Hydrogen atoms were refined following a riding model.

$[H_2L^3][PF_6]_2$. Crystals were obtained by slow diffusion of hexane into dichloromethane solutions of the $[H_2L^3][PF_6]_2$ salt. No absorption corrections were applied. The structure was solved using direct methods. Anisotropic thermal parameters were used for all non-hydrogen atoms. The H atoms of a water molecule were located on a Fourier-difference map. Hydrogen atoms were refined following a riding model.

[H_2L^4][PF_6]$_2$. Crystals were obtained by slow diffusion of hexane into dichloromethane solutions of the [H_2L^4][PF_6]$_2$ salt. ψ-Scan absorption corrections were applied (maximum and minimum transmission 0.585 and 0.570). The structure was solved using direct methods. Anisotropic thermal parameters were used for all non-hydrogen atoms. Hydrogen atoms were refined following a riding model. A solvent molecule (CH_2Cl_2) was found highly disordered near an inversion centre and refined isotropically with fixed C–Cl distances.

[H_2L^5][PF_6]$_2$. Crystals were obtained by slow diffusion of hexane into dichloromethane solutions of the [H_2L^5][PF_6]$_2$ salt. No absorption corrections were applied. The structure was solved using direct methods. Anisotropic thermal parameters were used for all non-hydrogen atoms. Hydrogen atoms were refined following a riding model.

CCDC reference number 186/1467.

See http://www.rsc.org/suppdata/dt/1999/2359/ for crystallographic files in .cif format.

Results and discussion

We have synthesized the cyclic and open-chain aza–oxa ferrocene-functionalised molecules L^1–L^5. Bearing in mind that aza–oxa macrocycles usually display selective co-ordination against large over small metal ions, receptors L^1–L^5 are prototypes suitable for study of the electrochemical sensing of large heavy toxic metal ions in aqueous environments. Receptors L^1 and L^5 have been published elsewhere. Compound L^1 was obtained by reaction of the corresponding aza–oxa derivative with the salt (ferrocenylmethyl)trimethylammonium iodide in acetonitrile in the presence of potassium carbonate. This has proved to be a suitable method to introduce ferrocenylmethyl frameworks to secondary amines. A similar procedure was followed to synthesize ligands L^3 and L^4. Functionalisation with ferrocenyl groups of primary amines can be adequately carried out by reaction of the appropriate amine with ferrocene-functionalised aldehydes. Following this procedure the receptor L^5 was synthesized by reaction of 2,2′-(ethylenedioxy)bis(ethylamine) with ferrocenecarbaldehyde and further reduction with $LiAlH_4$. In a similar manner L^2 was obtained by reaction of ferrocene-1,1′-dicarbaldehyde and 2,2′-(ethylenedioxy)bis(ethylamine) and further chemical reduction. The ^{1}H NMR, FAB mass spectra and elemental analysis were consistent with the proposed formulation.

An unexpected reaction between receptor L^4 and Cu^{2+} has also been found. In an attempt to obtain the Cu^{2+} complex of receptor L^4 we refluxed L^4 and Cu^{2+} in ethanol. Further addition of [NH_4][PF_6] gave a yellow solid that was characterised as [H_2L^5][PF_6]$_2$. This was not an expected reaction and implies the cleavage of C–N bonds. The reaction appears to be metal assisted, although also partial conversion of L^4 into L^5 can also be observed after refluxing L^4 in ethanolic solutions. Scheme 1 shows a reaction process. Unexpected rupture of C–N chemical bonds has also recently been reported in ferrocene derivatives.[30]

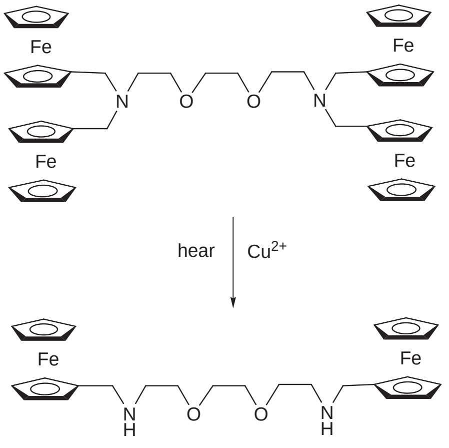

Scheme 1

Except L^3 that is a solid, L^1, L^2, L^4 and L^5 were waxy oils. However, L^1, L^3, L^4 and L^5 receptors can be obtained as solids by addition of [NH_4][PF_6] to ethanolic solutions of the corresponding receptors and further addition of water to give [HL^1][PF_6], [H_2L^3][PF_6]$_2$, [H_2L^4][PF_6]$_2$ and [H_2L^5][PF_6]$_2$. The crystal and molecular structures of these salts have been determined by single crystal X-ray procedures.

Crystal structures

Figs. 1, 2, 3 and 4 display views of the molecules showing the atomic numbering schemes, whereas Tables 2, 3, 4 and 5 show some selected bond distances and angles for the crystal structures of the [HL^1][PF_6], [H_2L^3][PF_6]$_2$, [H_2L^4][PF_6]$_2$ and [H_2L^5][PF_6]$_2$ salts, respectively. The structures consist of cationic protonated amines linked *via* ionic interactions with hexafluorophosphate anions. Additionally some hydrogen bonding interactions have also been found in the molecular structures of [H_2L^3][PF_6]$_2$, [H_2L^4][PF_6]$_2$ and [H_2L^5][PF_6]$_2$. Apart from the characterisation of the receptors the study of the hydrogen-bonding interactions found in the crystal gives some information of the effect of the bulky ferrocenyl groups and the presence of secondary or tertiary amines on the intermolecular interactions between protonated ammonium groups and electronegative atoms. Although this paper is mainly concerned with electrochemical cation sensing, it can be of importance to

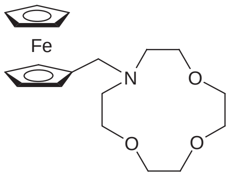

L^1

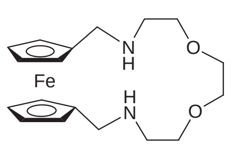

L^2

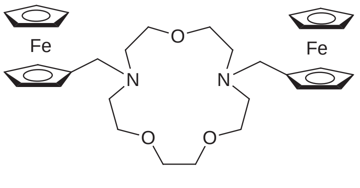

L^3

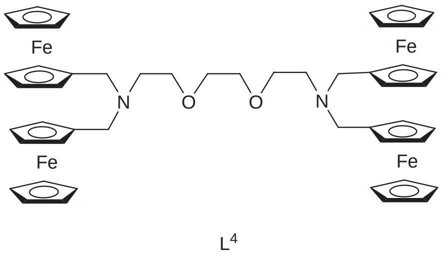

L^4

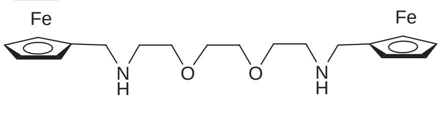

L^5

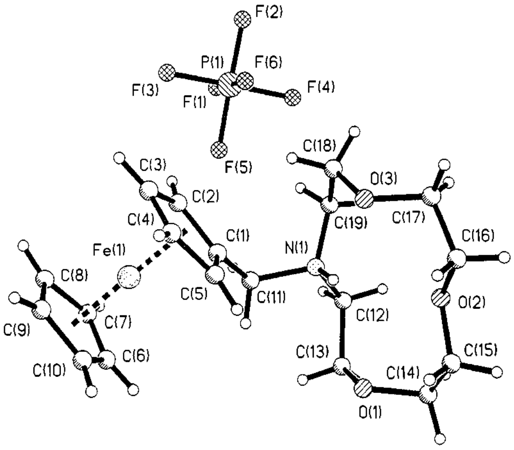

Fig. 1 Crystal structure of $[HL^1][PF_6]$.

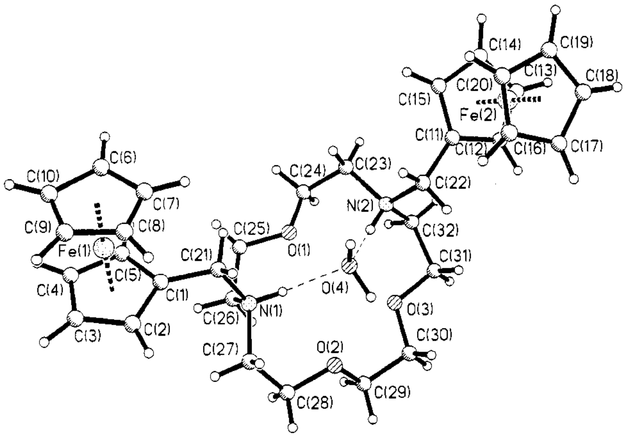

Fig. 2 Crystal structure of $[H_2L^3][PF_6]_2$.

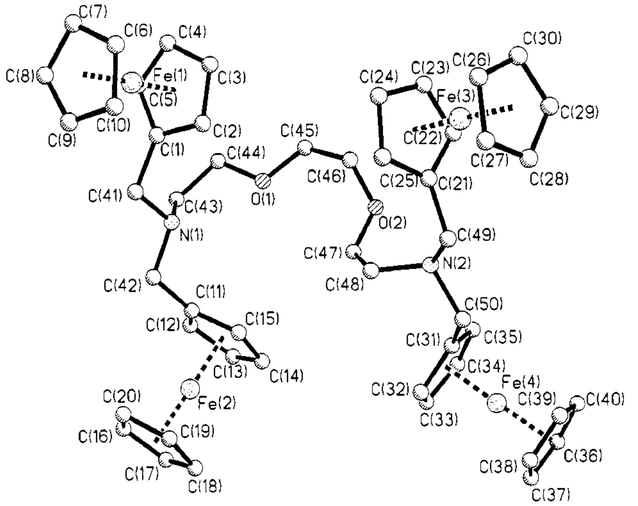

Fig. 3 Crystal structure of $[H_2L^4][PF_6]_2$.

look deeply into the cation–anion interaction in anion sensing receptors based on ferrocene-functionalised receptors. There is no electrostatic interaction between $[HL^1]^+$ and PF_6^- in the $[HL^1][PF_6]$ crystal structure. Hydrogen-bonding interactions however appear to be favoured in the open-chain receptor containing secondary N-donor atom, L^5. Fig. 4(a) shows the $[H_2L^5]^{2+}$ cation and the two non-equivalent PF_6^- anions, revealing the F(6) interaction with the hydrogen atoms of the ammonium groups; H···F(6) distances are 2.485(12) and 2.659(12) Å. The F(6) atom is 1.67 Å away from the mean plane O(1)–O(2)–N(1)–N(2). The position occupied by it is similar to that found for the water molecule in the $[H_2L^3][PF_6]_2$ crystal structure. Some intermolecular distances are given in Table 5, whereas Fig. 4(b) shows a more detailed view of the hydrogen-bonding network. Each $[H_2L^5]^{2+}$ shows intermolecular distances with four PF_6^- anions. Compound L^3 has a larger ring size than L^1 and hydrogen bonds have been found between a water molecule and the hydrogen atoms of the ammonium groups. Fig. 2 displays a view of the molecule emphasising the intermolecular oxygen–hydrogen interactions; O(4)···H(N1) 2.016(9) and O(4)···H(N2) = 2.147(10) Å.

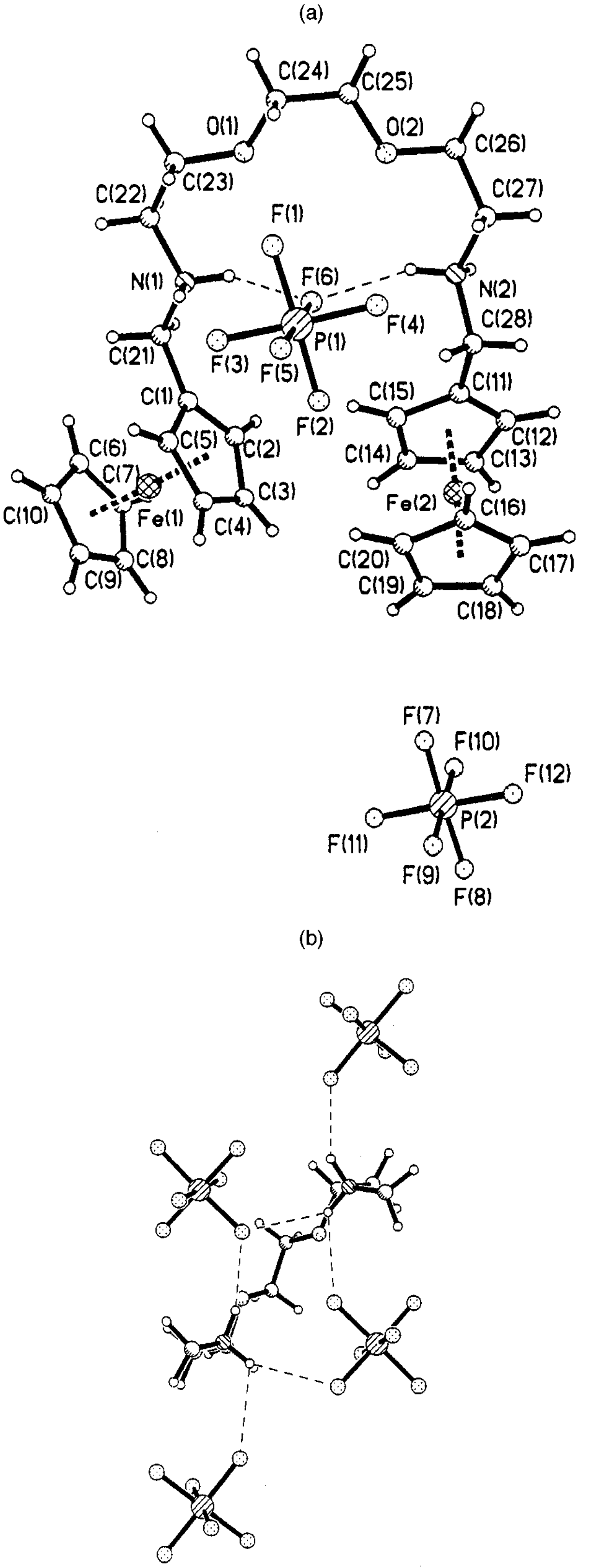

Fig. 4 Crystal structure of $[H_2L^5][PF_6]_2$.

Table 1 Crystallographic data for $[HL^1][PF_6]$, $[H_2L^3][PF_6]_2$, $[H_2L^4][PF_6]_2$ and $[H_2L^5][PF_6]_2$

	$[HL^1][PF_6]$	$[H_2L^3][PF_6]_2$	$[H_2L^4][PF_6]_2$	$[H_2L^5][PF_6]_2$
Formula	$C_{19}H_{28}F_6FeNO_3P$	$C_{33}H_{48}Cl_2F_{12}Fe_2N_2O_4P_2$	$C_{50.5}H_{58}ClF_{12}Fe_4N_2O_2P_2$	$C_{28}H_{38}F_{12}Fe_2N_2O_2P_2$
M	519.24	1009.27	1273.78	835.92
Crystal system	Monoclinic	Triclinic	Triclinic	Orthorhombic
Space group	$P2_1$	$P\bar{1}$	$P\bar{1}$	$Pbcn$
a/Å	8.049(3)	11.069(4)	13.956(3)	41.858(8)
b/Å	10.353(4)	11.206(4)	14.524(2)	9.543(3)
c/Å	13.905(6)	17.482(6)	16.619(2)	16.801(5)
α/°		85.12(3)	67.298(10)	
β/°	104.24(3)	75.06(3)	65.209(12)	
γ/°		87.18(3)	69.930(13)	
V/Å^3	1123.2(7)	2086.7(13)	2754.3(8)	6712(3)
Z	2	2	2	8
T/°C	20	20	20	20
Reflections collected	3172	5702	7444	4389
Independent reflections	2925	5359	7086	4389
μ/cm^{-1}	8.12	9.92	12.20	10.57
$R1$ ($F > 4\sigma(F)$)	0.052	0.071	0.102	0.065
$wR2$ (all data)	0.150	0.210	0.283	0.202

Table 2 Selected bond lengths (Å) and angles (°) for compound $[HL^1][PF_6]$

N(1)–C(19)	1.476(11)	N(1)–C(11)	1.510(10)
N(1)–C(12)	1.515(10)	O(1)–C(13)	1.415(11)
O(1)–C(14)	1.432(10)	O(2)–C(15)	1.400(11)
O(2)–C(16)	1.451(11)	O(3)–C(18)	1.401(13)
C(1)–C(5)	1.423(11)	C(1)–C(11)	1.469(11)
C(12)–C(13)	1.499(13)	C(14)–C(15)	1.462(13)
Average Fe(1)–C (Cp ring)	2.025(10)		
C(19)–N(1)–C(12)	110.7(7)	C(11)–N(1)–C(12)	110.7(6)
C(13)–O(1)–C(14)	115.7(7)	C(15)–O(2)–C(16)	114.5(8)
C(18)–O(3)–C(17)	122.6(10)	C(13)–C(12)–N(1)	113.2(7)

Table 3 Selected bond lengths (Å) and angles (°) for compound $[H_2L^3][PF_6]_2$

N(1)–C(26)	1.496(9)	N(1)–C(21)	1.504(9)
N(1)–C(27)	1.518(9)	N(2)–C(32)	1.492(9)
N(2)–C(23)	1.501(9)	N(2)–C(22)	1.529(8)
O(1)–C(24)	1.411(9)	O(1)–C(25)	1.423(9)
O(2)–C(29)	1.402(10)	O(2)–C(28)	1.419(9)
O(3)–C(30)	1.413(9)	O(3)–C(31)	1.418(8)
Average Fe(1)–C (Cp ring)	2.029(11)	Fe(2)–C (Cp ring)	2.030(12)
O(4) $\cdots$ H(N1)	2.016(9)	O(4) $\cdots$ H(N2)	2.147(10)
H1(O4) $\cdots$ O(2)	2.389(11)	H1(O4) $\cdots$ F(9)	2.204(10)
H2(O4) $\cdots$ F(12)	2.241(12)	H2(O4) $\cdots$ F(16)	1.792(8)
C(26)–N(1)–C(21)	114.3(6)	C(26)–N(1)–C(27)	112.5(6)
C(21)–N(1)–C(27)	110.0(6)	C(32)–N(2)–C(23)	113.9(6)
C(32)–N(2)–C(22)	113.4(5)	C(23)–N(2)–C(22)	110.5(6)
C(24)–O(1)–C(25)	113.6(6)	C(29)–O(2)–C(28)	112.9(7)
C(30)–O(3)–C(31)	114.1(6)		

Table 4 Selected bond lengths (Å) and angles (°) for compound $[H_2L^4][PF_6]_2$

N(1)–C(41)	1.48(2)	N(1)–C(42)	1.51(2)
N(1)–C(43)	1.52(2)	N(2)–C(48)	1.47(2)
N(2)–C(49)	1.52(2)	N(2)–C(50)	1.56(2)
O(1)–C(45)	1.41(2)	O(1)–C(44)	1.42(2)
O(2)–C(47)	1.39(2)	O(2)–C(46)	1.41(2)
Average Fe(1)–C (Cp ring)	2.02(2)	Fe(2)–C (Cp ring)	2.05(2)
Average Fe(3)–C (Cp ring)	2.03(2)	Fe(4)–C (Cp ring)	2.03(2)
H(N1) $\cdots$ F(6)	2.31(2)	H(N2) $\cdots$ F(12)	2.31(2)
C(41)–N(1)–C(42)	109.9(12)	C(41)–N(1)–C(43)	115.2(13)
C(42)–N(1)–C(43)	108.4(13)	C(48)–N(2)–C(49)	113.6(12)
C(48)–N(2)–C(50)	113.4(12)	C(49)–N(2)–C(50)	108.2(11)
C(45)–O(1)–C(44)	113.8(13)	C(47)–O(2)–C(46)	117(2)

Table 5 Selected bond lengths (Å) and angles (°) for compound $[H_6L^5][PF_6]_2$

N(1)–C(22)	1.480(11)	N(1)–C(21)	1.507(11)
N(2)–C(28)	1.488(12)	N(2)–C(27)	1.491(11)
O(1)–C(23)	1.415(12)	O(1)–C(24)	1.429(11)
O(2)–C(26)	1.394(13)	O(2)–C(25)	1.396(13)
Average Fe(1)–C (Cp ring)	2.028(10)	Fe(2)–C (Cp ring)	2.033(10)
H1(N1) $\cdots$ F(3)	2.434(11)	H1(N1) $\cdots$ F(10)	2.513(12)
H2(N1) $\cdots$ F(6)	2.485(12)	H2(N1) $\cdots$ F(9)	2.431(10)
H1(N2) $\cdots$ F(6)	2.659(12)	H1(N2) $\cdots$ F(9)	2.155(10)
H2(N2) $\cdots$ F(5)	2.174(11)	H2(N2) $\cdots$ F(12)	2.635(13)
C(22)–N(1)–C(21)	112.7(8)	C(28)–N(2)–C(27)	114.6(8)
C(23)–O(1)–C(24)	113.8(8)	C(26)–O(2)–C(25)	113.4(9)

Atom O(4) of the water molecule is 2.02 Å away from the mean plane defined by the O(1)–O(2)–O(3)–O(4) atoms. The presence of tertiary amines in L^4 in contrast with the existence of secondary ones in L^5 and the presence of two bulky ferrocenyl groups around each ammonium group in L^4 induces the existence of a lesser number of hydrogen bonding interactions when compared to the intermolecular bond distances between the crystal structures of the two open-chain receptors $[H_2L^4][PF_6]_2$ and $[H_2L^5][PF_6]_2$. Intermolecular distances were found between the hydrogen atoms of the ammonium groups and the F(6) and F(12) atoms, 2.31(2) Å.

Potentiometric cation binding studies

Potentiometric studies have been carried out in an attempt to provide some explanation of the observed electrochemical behaviour (see below) and to find a connection between the receptor–substrate interaction at the molecular level and the observed macroscopic electrochemical signal. Potentiometric techniques allow one to deduce which species are responsible for the oxidation potential shift of the ferrocenyl groups at a certain pH, and these studies can be of importance in an attempt to rationalise the sensing behaviour of the electroactive receptors in aqueous environments.

Solution studies directed to the determination of protonation constants and stability constants for the formation of complexes of L^1, L^2, L^3 and L^5 with transition metal ions have been carried out. Data for L^1 and L^2 have been obtained in water (25 °C, 0.1 mol dm^{-3} potassium perchlorate), whereas data for L^3 and L^5 have been determined in 1,4-dioxane–water (70 : 30 v/v, 25 °C, 0.1 mol dm^{-3} potassium nitrate) due to their low solubility in water over a wide pH range. Protonation constants

Table 6 Stepwise protonation constants for L^1, L^2, L^3, L^4 and L^5. Water (25 °C, 0.1 mol dm^{-3} potassium perchlorate) was used for L^1 and L^2 and 1,4-dioxane–water (70 : 30 v/v, 25 °C, 0.1 mol dm^{-3} potassium nitrate) for L^3, L^4 and L^5

Reaction	L^1	L^2	L^3	L^4	L^5
$L + H \rightleftharpoons HL$[a]	9.40(2)[b]	9.44(2)	8.40(2)	7.88(1)	8.83(2)
$L + 2H \rightleftharpoons H_2L$		17.32(2)	15.09(3)	14.58(1)	16.49(2)
$HL + H \rightleftharpoons H_2L$		7.88	6.69	6.7	7.66

[a] Charges have been omitted for clarity. [b] Values in parentheses are the standard deviations in the last significant digit.

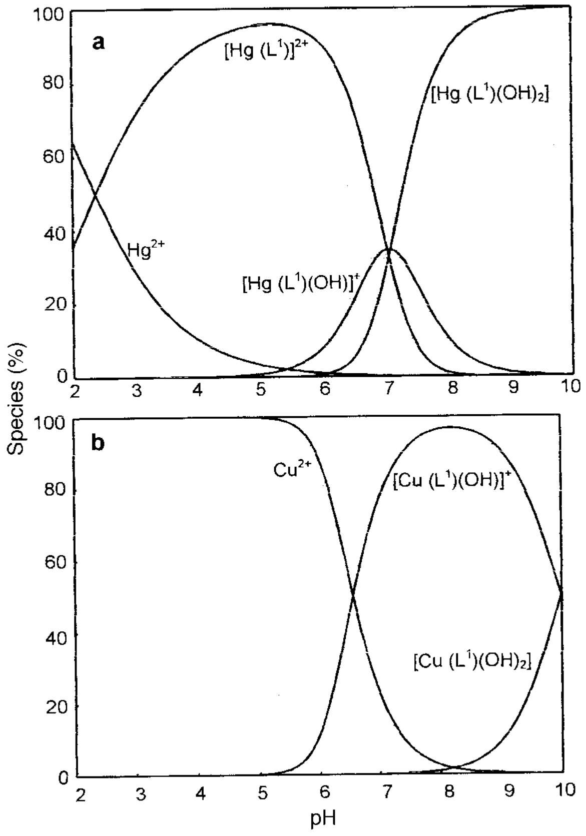

Fig. 5 Distribution diagrams of the (a) L^1–H^+–Hg^{2+} and (b) L^1–H^+–Cu^{2+} systems.

of receptors L^1 to L^5 are shown in Table 6. Protonation constants of L^1 and L^2 have values close to that reported for the analogous non-functionalised receptors in water,[31,32] however the use of 1,4-dioxane–water (70 : 30 v/v) slightly reduces the values of the first protonation processes for receptors L^3, L^4 and L^5 compared to those of L^1 and L^2 in water. This reduction of the first protonation process when compared with the same process in water has also been reported previously.[22]

The formation constants of the complexes between L^1, L^2, L^3 and L^5 and Cu^{2+}, Zn^{2+}, Cd^{2+}, Pb^{2+} and Hg^{2+} are shown in Tables 7, 9, 10 and 11. All the receptors form stable complexes with all the metal ions studied. Receptor L^1 forms more stable complexes with Hg^{2+} that with other metal ions studied. This is reflected in the existence of the $[Hg(L^1)]^{2+}$ species, whereas the remaining metal ions except Pb^{2+} only form hydroxo species, indicating how strongly water competes with these metal ions in the co-ordination process to the macrocyclic cavity. Additionally distribution diagrams show that Hg^{2+} forms complexes at more acid pH than the remaining metal ions as it can be observed in Fig. 5 which shows the distribution diagrams for the L^1–H^+–Hg^{2+} and L^1–H^+–Cu^{2+} systems, respectively. Selectivity and therefore the determination of the prevailing species in a complex mixture can be calculated from ternary distribution diagrams. The ternary diagrams have been calculated for the systems L–Hg^{2+}–M^{2+} ($M^{2+} = Cu^{2+}$, Zn^{2+}, Cd^{2+}, or Pb^{2+}) to show the competition between Hg^{2+} and M^{2+} (equimolar amounts) to interact with L^1. All these diagrams clearly display a complete selectivity for Hg^{2+} over the remaining metal ions. The functionalisation with a ferrocenyl group does not appear to modify the co-ordination behaviour of the oxa–aza cavity taking into account that the 1,4,7-trioxa-10-azacyclododecane receptor also displays larger formation constants with Hg^{2+} than with other common metal ions.[32] We have also determined the stability constants of the complexes between L^1 and Cu^{2+}, Cd^{2+}, Pb^{2+} and Hg^{2+} in the presence of a concentration of 4×10^{-3} mol dm^{-3} of Cl^- (see Table 8). This has been mainly done to study the effect that the presence of anions has on the electrochemical behaviour of transition metal complexes (see below). There is no important change in the stability constant values of the L–H^+–M^{2+} systems when $M^{2+} = Cu^{2+}$, Cd^{2+} or Pb^{2+}, but a significant decrease of the co-ordination ability of L^1 against Hg^{2+} is found in the presence of Cl^-.

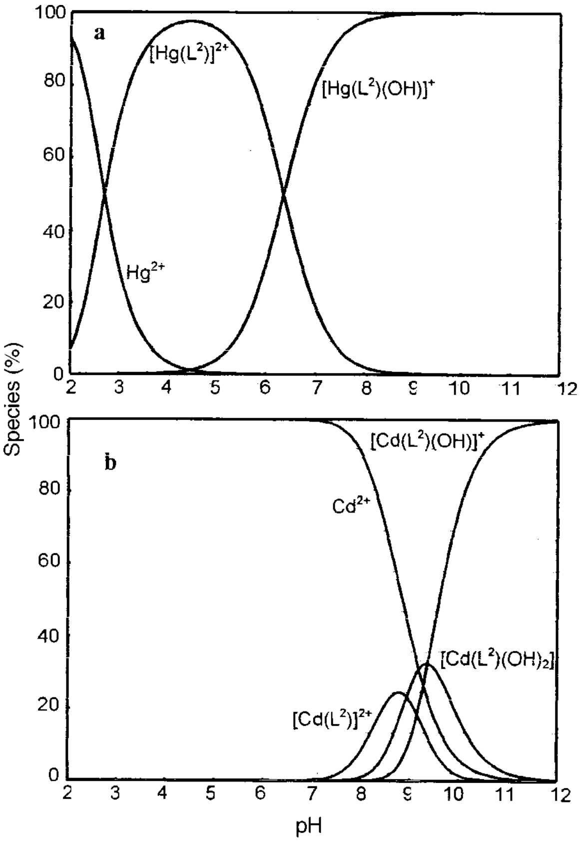

Fig. 6 Distribution diagrams of the (a) L^2–H^+–Hg^{2+} and (b) L^2–H^+–Cd^{2+} systems.

Receptor L^2 also shows a large affinity for Hg^{2+}, which is reflected in the stability constant values. Fig. 6 shows the distribution diagrams of the L^2–H^+–Hg^{2+} and L^2–H^+–Cd^{2+} systems. The stability constants for the formation of Cu^{2+}, Zn^{2+}, Cd^{2+}, Pb^{2+} and Hg^{2+} complexes of receptor L^3 in 1,4-dioxane–water (70 : 30 v/v, 0.1 mol dm^{-3} potassium nitrate) are shown in Table 10. The complexes $[M(HL^3)]^{3+}$, $[M(L^3)]^{2+}$, $[M(L^3)(OH)]^+$ and $[M(L^3)(OH)_2]$ have been found to exist for Cd^{2+}, Pb^{2+} and Hg^{2+}. The values of the stability constants of the $[M(L^3)]^{2+}$ species are in the sequence $Cd^{2+} = Cu^{2+} = Pb^{2+} < Hg^{2+}$. However although Hg^{2+} has a larger stability constant for the equilibrium $L^3 + Hg^{2+} \rightleftharpoons [Hg(L^3)]^{2+}$ the difference with respect to the same reaction for Cu^{2+}, Cd^{2+} or Pb^{2+} is not as high as when L^1 or L^2 is used as receptor. Receptor L^5 shows the same trend for selective complexation against Hg^{2+} over Ni^{2+}, Zn^{2+} and Cd^{2+}.

Electrochemical cation recognition investigations

Probably the most interesting feature in receptors L^1 to L^5 is the

Table 7 Stability constants (log *K*) for the formation of Cu^{2+}, Zn^{2+}, Cd^{2+}, Pb^{2+} and Hg^{2+} complexes of L^1 in water at 25 °C in 0.1 mol dm^{-3} $KClO_4$

Reaction	Cu^{2+}	Zn^{2+}	Cd^{2+}	Pb^{2+}	Hg^{2+}
$M^{2+} + L^1 \rightleftharpoons [M(L^1)]^{2+}$	—	—	—	5.29(5)[a]	10.03(4)
$M^{2+} + L^1 + H_2O \rightleftharpoons [M(L^1)(OH)]^+ + H^+$	−0.72(2)	−3.49(3)	−6.19(2)	−3.47(7)	3.0(1)
$M^{2+} + L^1 + 2H_2O \rightleftharpoons [M(L^1)(OH)_2] + 2H^+$	−10.10(4)	−13.10(4)	−16.52(2)	−13.23(6)	−4.08(7)

[a] Values in parentheses are standard deviations on the last significant figure.

Table 8 Stability constants (log *K*) for the formation of Cu^{2+}, Cd^{2+}, Pb^{2+} and Hg^{2+} complexes of L^1 (in the presence of a concentration of 4×10^{-3} mol dm^{-3} of Cl^-) in water at 25 °C in 0.1 mol dm^{-3} $KClO_4$

Reaction	Cu^{2+}	Cd^{2+}	Pb^{2+}	Hg^{2+}
$M^{2+} + L^1 \rightleftharpoons [M(L^1)]^{2+}$			5.35(5)	5.7(1)
$M^{2+} + L^1 + H_2O \rightleftharpoons [M(L^1)(OH)]^+ + H^+$	−1.00(4)	−5.99(6)	−3.08(5)	−2.03(5)
$M^{2+} + L^1 + 2H_2O \rightleftharpoons [M(L^1)(OH)_2] + 2H^+$	−9.97(6)	−16.24(4)	−12.97(5)	−12.02(6)

[a] Values in parentheses are standard deviations on the last significant figure.

Table 9 Stability constants (log *K*) for the formation of Cu^{2+}, Zn^{2+}, Cd^{2+}, Pb^{2+} and Hg^{2+} complexes of L^2 in water at 25 °C in 0.1 mol dm^{-3} $KClO_4$

Reaction	Cu^{2+}	Zn^{2+}	Cd^{2+}	Pb^{2+}	Hg^{2+}
$M^{2+} + L^2 + H^+ \rightleftharpoons [M(HL^2)]^{3+}$				12.65(9)[a]	
$M^{2+} + L^2 \rightleftharpoons [M(L^2)]^{2+}$	7.22(2)	4.68(5)	3.42(5)	6.23(1)	14.94(2)
$M^{2+} + L^2 + H_2O \rightleftharpoons [M(L^2)(OH)]^+ + H^+$	−0.87(2)	−3.01(2)	−5.51(4)	−1.73(2)	8.57(3)
$M^{2+} + L^2 + 2H_2O \rightleftharpoons [M(L^2)(OH)_2] + 2H^+$	−10.73(3)	−12.34(2)	−14.87(3)	−10.81(2)	

[a] Values in parentheses are standard deviations on the last significant figure.

Table 10 Stability constants (log *K*) for the formation of Cu^{2+}, Zn^{2+}, Cd^{2+}, Pb^{2+} and Hg^{2+} complexes of L^3 in 1,4-dioxane–water (70 : 30 v/v, 25 °C, 0.1 mol dm^{-3} potassium nitrate)

Reaction	Cu^{2+}	Zn^{2+}	Cd^{2+}	Pb^{2+}	Hg^{2+}
$M^{2+} + L^3 + H^+ \rightleftharpoons [M(HL^3)]^{3+}$	—	—	12.35(5)[a]	12.45(4)	14.64(2)
$M^{2+} + L^3 \rightleftharpoons [M(L^3)]^{2+}$	6.27(2)	—	6.1(2)	6.43(2)	8.79(2)
$M^{2+} + L^3 + H_2O \rightleftharpoons [M(L^3)(OH)]^+ + H^+$	−0.37(2)	−2.88(1)	−3.17(5)	−1.94(2)	1.24(2)
$M^{2+} + L^3 + 2H_2O \rightleftharpoons [M(L^3)(OH)_2] + 2H^+$	−8.72(3)	−11.46(2)	−12.81(3)	−11.39(2)	−7.88(3)

[a] Values in parentheses are standard deviations on the last significant figure.

Table 11 Stability constants (log *K*) for the formation of Ni^{2+}, Zn^{2+}, Cd^{2+} and Hg^{2+} complexes of L^5 in 1,4-dioxane–water (70 : 30 v/v, 25 °C, 0.1 mol dm^{-3} potassium nitrate)

Reaction	Ni^{2+}	Zn^{2+}	Cd^{2+}	Hg^{2+}
$M^{2+} + L^5 + H^+ \rightleftharpoons [M(HL^5)]^{3+}$	—	—	12.59(4)[a]	15.54(3)
$M^{2+} + L^5 \rightleftharpoons [M(L^5)]^{2+}$	—	5.14(1)	4.73(3)	8.09(3)
$M^{2+} + L^5 + H_2O \rightleftharpoons [M(L^5)(OH)]^+ + H^+$	−4.07(2)	−3.21(1)	−4.10(2)	−1.37(5)
$M^{2+} + L^5 + 2H_2O \rightleftharpoons [M(L^5)(OH)_2] + 2H^+$	−12.2(1)	−13.24(4)	−14.79(4)	—

[a] Values in parentheses are standard deviations on the last significant figure.

presence near co-ordination sites of redox-active groups which can be affected by the presence of metal ions and transform chemical information at the molecular level (the presence or not of a target receptor) into a macroscopic signal easily measurable (variation of the oxidation potential shift of the redox-active groups). An electrochemical study has been carried out with the aim of detecting pH ranges of selectivity for electrochemical detection of heavy toxic metal ions such as Hg^{2+}. The potentiometric cation binding studies indicate that Hg^{2+} forms more stable complexes than other common metal ions with receptors L^1, L^2, L^3 and L^5, and the electrochemical studies were carried out with the hope that this favourable complexation of Hg^{2+} over Cu^{2+}, Zn^{2+}, Cd^{2+} and Pb^{2+} would be reflected in a selective electrochemical response.

The shift of the oxidation potential of the redox-active groups as a function of the pH in the presence and absence of Cu^{2+}, Zn^{2+}, Cd^{2+}, Pb^{2+} and Hg^{2+} was monitored in water (25 °C, 0.1 mol dm^{-3} potassium perchlorate) for receptors L^1 and L^2 and in 1,4-dioxane–water (70 : 30 v/v, 25 °C, 0.1 mol dm^{-3} potassium nitrate) for L^3, L^4 and L^5. The $E_{1/2}$ (from rde (rotating disk electrode) techniques) *vs.* pH curves for the systems $L–H^+–M^{2+}$ ($L = L^1, L^2, L^3, L^4$ or L^5; $M^{2+} = Cu^{2+}, Zn^{2+}, Cd^{2+}, Pb^{2+}$ or Hg^{2+}) with a ligand-to-metal molar ratio = 1 : 1 have been determined. Fig. 7 displays the electrochemical response found for receptors L^1 to L^5 as a function of the pH in the presence of metal ions ($\Delta E_{1/2}$ is defined at a certain pH as $E_{1/2}$(cation–receptor) − $E_{1/2}$(receptor); $E_{1/2}$ = half-wave potential from rde techniques).

Except ligand L^4 that does not show any important electrochemical shift upon addition of metal ions, the receptors L^1, L^2, L^3 and L^5 show significant shifts of the oxidation potential of the ferrocenyl groups upon addition of metal ions, especially for Hg^{2+}. Some other metal ions produce shifts of the oxidation potential of the ferrocenyl groups but these are smaller than the

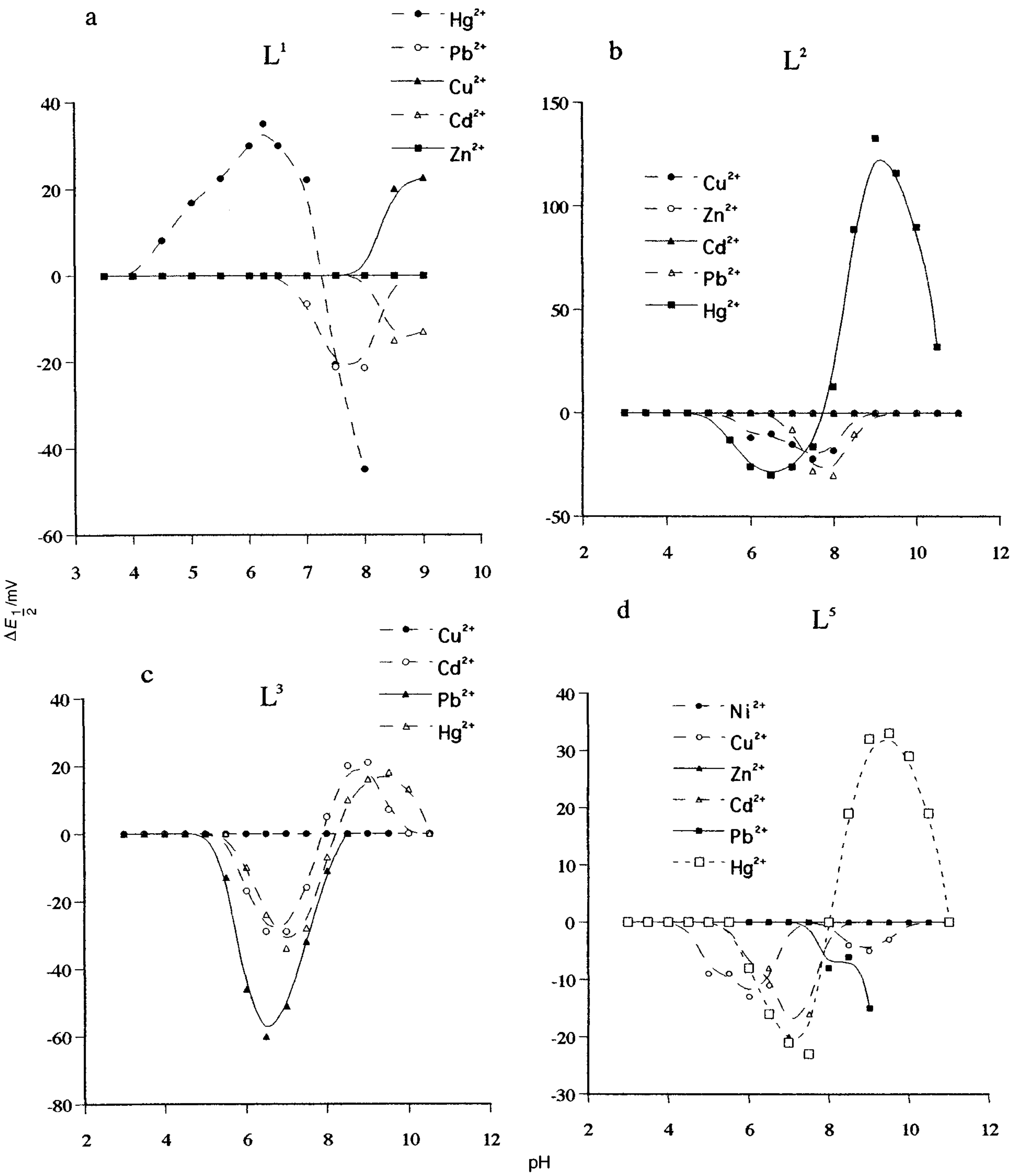

Fig. 7 Redox potential shift ($\Delta E_{1/2}$) for (a) L^1, (b) L^2, (c) L^3 and (d) L^5 in the presence of metal ions as a function of the pH.

electrochemical shift observed for mercury (except for L^3). Also important is the fact that the electrochemical sensing of Hg^{2+} is produced at pH ranges where other common metal ions do not produce any significant oxidation potential shift. Receptor L^3 shows the largest oxidation potential shifts upon addition of Pb^{2+}, although other large metal ions such as Cd^{2+} and Hg^{2+} also produce significant shifts. Different receptors can be chosen to select both the pH range where Hg^{2+} can be recognised and the nature of the shift (cathodic or anodic) with respect to $E_{1/2}$ of the free receptor upon addition of Hg^{2+}. For instance L^1 is able electrochemically to detect Hg^{2+} anodically at pH 6 and cathodically at pH 8. Also anodic and cathodic electrochemical shifts upon addition of Hg^{2+} have been found for receptors L^2, L^3 and L^5 at pH *ca.* 9 and *ca.* 7, respectively. The electrochemical response against Hg^{2+} is selective and approximately the same electrochemical shifts were observed upon addition of Hg^{2+} independently of the presence or not of other metal ions. This is consistent with the ternary diagrams which show that in a mixture of metal ions the receptors bind selectively Hg^{2+} over other M^{2+} ions studied. Of importance is the large electrochemical shift found in aqueous environments. For instance the presence of Hg^{2+} modifies the oxidation potential of the ferrocenyl group in L^2 anodically up to 130 mV, which is one of the largest shifts ever reported in electrochemical cation sensing behaviours in water using related receptors. This electrochemical selective sensing of Hg^{2+} strongly suggests the potential use of similar systems in the development of amperometric electrochemical methods or sensing devices for the selective determination of toxic heavy metal ions in water.

An important aspect is the relation between the existing species in solution and the electrochemical response.[11,12] From the comparison between potentiometric and electrochemical results it can clearly be concluded that Hg^{2+}, which is the metal ion that showed larger stability constants with receptors L^1, L^2, L^3 and L^5, also displays the largest electrochemical shift in electrochemical experiments (except for L^3). It appears that a selective electrochemical response against a target metal ion, at least for some cases, is found when (i) there are pH ranges of selective complexation or (ii) there are strong predominant receptor–metal complexes in a wide pH range. Fig. 5 shows the distribution diagram of the L^1–H^+–Hg^{2+} and L^1–H^+–Cu^{2+} systems. It reveals that when the $[Hg(L^1)]^{2+}$ complex is predominant there is no interaction between L^1 and any other metal ion studied. Therefore there is a pH range (2.5–7) of selective complexation of Hg^{2+}. This is related with the high affinity of Hg^{2+} for L^1 and therefore the reaction $Hg^{2+} + [HL^1]^+ \rightleftharpoons [Hg(L^1)]^{2+} + H^+$ is observed a lower pH value than when other metal ions are used. The presence of strong receptor metal complexes in a wide pH range also induces large electrochemical shifts. This can be observed when we compare the electrochemical behaviour and the distribution diagrams of the L^2–H^+–Hg^{2+} and L^2–H^+–Cd^{2+} systems. In the L^2–H^+–Hg^{2+} system the complex $[Hg(L^1)(OH)]^+$ is predominant in the pH range 6.5–10 and therefore it would be expected that the oxidation potential of the ferrocenyl groups would not change over the same pH range. In fact the oxidation potential of the L^2–H^+–Hg^{2+} system remains almost without variation in the pH range 6–9 (see below).

In considering the relation between the receptor–substrate interaction at the molecular level and the macroscopic electrochemical signal one should be aware of the nature of the interaction process between the ferrocene group and the metal ion. For receptors such as L^1 to L^5 there is a lack of any electron delocalisation path between the ferrocenyl groups and the donor atoms through the organic groups attached to them and therefore the interaction between the guest and the redox-active group has to be mainly electrostatic. The nature of the binding sites controls the selectivity against certain metal ions, whereas the ferrocene group is able to transform the charge of the complex into a macroscopically measurable electrochemical shift. The supposition is that when at a certain pH there is a difference between the charge of the free receptor and the charge of the complex then an electrochemical shift would be observed. The shift will be anodic or cathodic depending on whether the charge of the complex is larger than that of the free receptor or the charge of the free receptor is larger than that of the complex, respectively. This gives in some cases an easy tool roughly to predict electrochemical behaviours. One proof that the above statements are basically true is that the electrochemical behaviour of the receptors L^1 and L^2 towards transition metal ions can be roughly predicted from potentiometric data. The charge of the complex at a certain pH can be predicted from the distribution diagrams of the different L–H^+–M^{2+} systems which give the percentage of each species at a certain pH; Z_{av} (average charge) is defined as $\Sigma x_i z_i$, where x_i and z_i are the molar fraction and the charge of the existing species at a determined pH. Fig. 8 shows a comparison between the experimental $E_{1/2}$ *vs.* pH and Z_{av} *vs.* pH curves for the L^1–H^+, L^1–H^+–Hg^{2+} and L^1–H^+–Cu^{2+} systems, Fig. 9 that for the L^2–H^+, L^2–H^+–Hg^{2+} and L^2–H^+–Cd^{2+} systems. As it can be observed there is a satisfactory agreement between the observed and predicted curves. However we have not found such a good correlation between experimental and calculated curves for the receptors L^3 and L^5. Although the reason for this is not clear it can be related with the fact that the electrostatic interpretation stated above is quite plain and does not take into account potential structural variation of the different species in solution, possible changes of ferrocene–cation distances as a function of the pH, *etc.*

The shift of the oxidation potential of the redox-active groups as a function of the pH in the presence and absence of Cu^{2+}, Zn^{2+}, Cd^{2+}, Pb^{2+} and Hg^{2+} was also monitored in water (25 °C, 0.1 mol dm^{-3} potassium perchlorate) for receptor L^1 in the presence of chloride anions ($[Cl^-] = 4 \times 10^{-3}$ mol dm^{-3}). This has been mainly done to check the potential use in anion sensing by ferrocene-containing complexes. Although there are not too many investigations on the electrochemical sensing of anions in aqueous environments, some studies have been based on polyammonium receptors functionalised with ferrocenyl groups,[4,13] ferrocenyl-based thiourea and guanidinium receptors[18] or ferrocenylboronic derivatives.[9,14] In all cases the recognition process includes anion–ligand interactions, but to the best of our knowledge no studies have been carried out dealing with the use of redox-active complexes for the electrochemical recognition of anions.

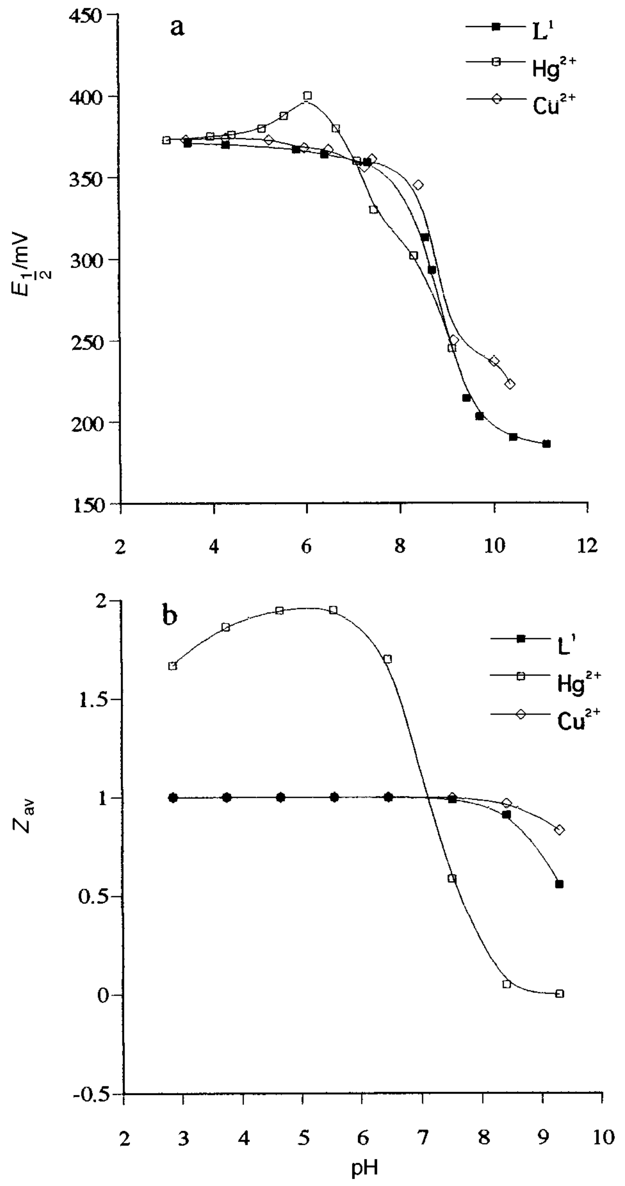

Fig. 8 (a) $E_{1/2}$ *vs.* pH and (b) Z_{av} *vs.* pH curves for L^1–H^+, L^1–H^+–Hg^{2+} and L^1–H^+–Cu^{2+}.

Curves of $E_{1/2}$ (from rde techniques) *vs.* pH for the systems L^1–H^+–M^{2+} ($M^{2+} = Cu^{2+}$, Zn^{2+}, Cd^{2+}, Pb^{2+} or Hg^{2+}) with a ligand-to-metal molar ratio = 1 : 1 and in the presence of $[Cl^-] = 4 \times 10^{-3}$ mol dm^{-3} have been determined. Fig. 10 displays the electrochemical response as a function of the pH ($\Delta E_{1/2}$ defined as $E_{1/2}$(cation–receptor) − $E_{1/2}$/(receptor)). As it can be observed there is a considerable change of L^1 response against Hg^{2+} in Fig. 10 when compared with Fig. 7(a) due to the presence of Cl^-. This suggest that the Hg^{2+} complex of L^1 could act as a receptor for the electrochemical sensing of chloride. Fig. 11 shows the electrochemical response against

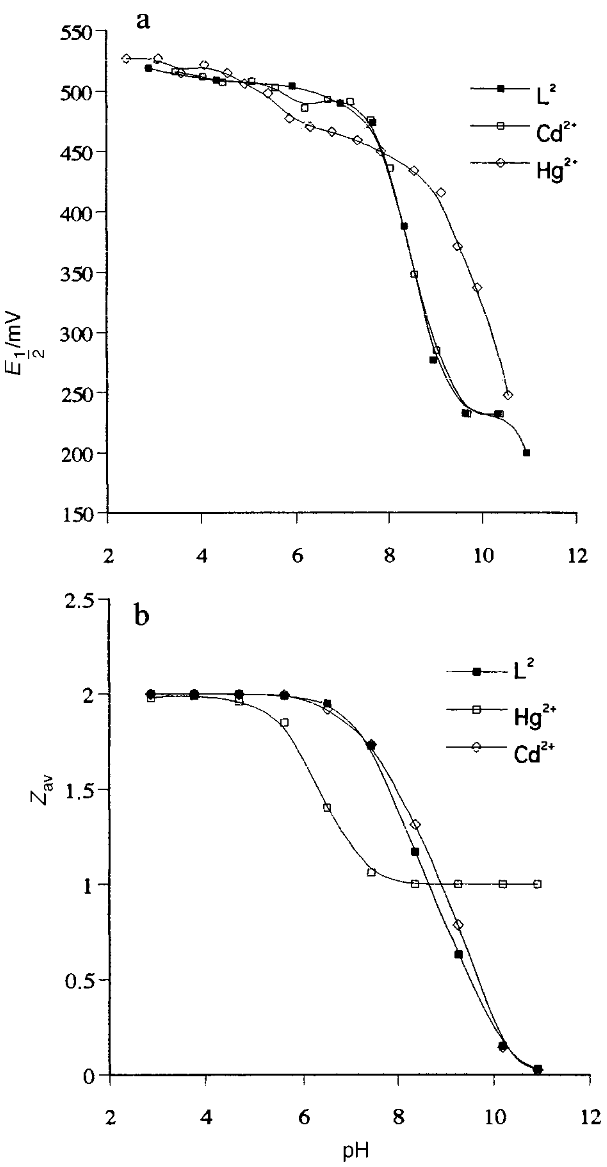

Fig. 9 (a) $E_{1/2}$ *vs.* pH and (b) Z_{av} *vs.* pH curves for L^2–H^+, L^2–H^+–Hg^{2+} and L^2–H^+–Cd^{2+}.

Cl^- ($\Delta E_{1/2}$ at a certain pH is defined as $E_{1/2}(L^1\text{–}Hg^{2+}) - E_{1/2}(L^1\text{–}Hg^{2+}\text{–}Cl^-)$). There is a significant shift around pH 7 of near 60 mV.

Conclusions

A combination of well known co-ordination properties and suitable redox groups has proved a good method strategically to design new receptors for the electrochemical recognition of Hg^{2+} in aqueous solution. The strategy has included the selection of suitable binding sites such as aza–oxa derivatives and functionalisation with ferrocenyl groups. Both open-chain and cyclic architectures have been designed. Selective co-ordination ability against Hg^{2+} has been found using potentiometric techniques which is reflected in the electrochemical studies. Selective electrochemical sensing of Hg^{2+} in water has been found. Large electrochemical shifts up to 130 mV were produced upon addition of Hg^{2+} suggesting a potential application in the development of the amperometric detection of such a heavy toxic metal cation selectively over other common water-present cations. Additionally the potential use of metal complexes containing an electroactive group as sensing receptors of anions has also been pointed out. The complex $[Hg(L^1)]^{2+}$ is able electrochemically to recognise Cl^- in water at neutral pH.

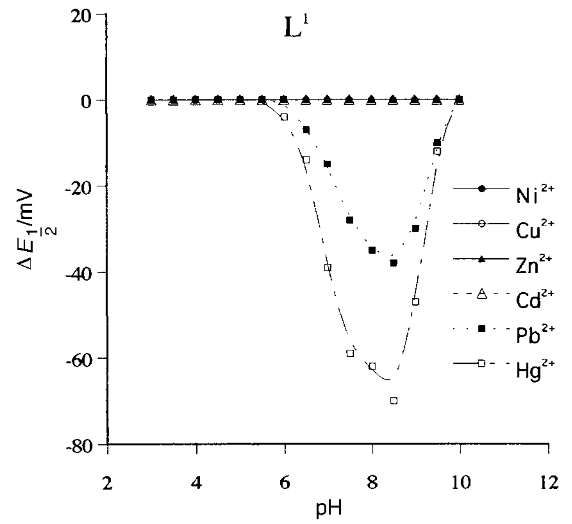

Fig. 10 Redox potential shift ($\Delta E_{1/2}$) for L^1 in the presence of Ni^{2+}, Cu^{2+}, Zn^{2+}, Cd^{2+}, Pb^{2+} and Hg^{2+} and $[Cl^-] = 4 \times 10^{-3}$ mol dm^{-3}, as a function of the pH.

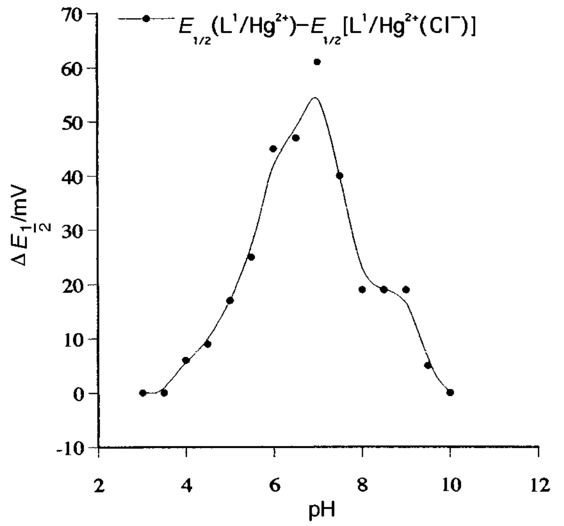

Fig. 11 Redox potential shift ($\Delta E_{1/2}$) as a function of the pH.

Acknowledgements

We should like to thank the Dirección General de Investigación Científica y Técnica (proyecto PB95-1121-C02-02) for support. We also thank the EPSRC and British Petroleum for studentships (J. C., D. K. S.) and the EPSRC for use of the mass spectrometry service at University College Swansea.

References

1 P. D. Beer, *Chem. Soc. Rev.*, 1989, **18**, 409; *Adv. Inorg. Chem.*, 1992, **39**, 79; *Acc. Chem. Res.*, 1998, **31**, 71.
2 A. W. Czarnik, *Acc. Chem. Res.*, 1994, **27**, 302; V. Balzani and F. Scandola, *Supramolecular Photochemistry*, Ellis Horwood, Chichester, 1991.
3 J. C. Medina, T. T. Goodnow, M. T. Rojas, J. L. Atwood, B. C. Lynn, A. E. Kaifer and G. W. Gokel, *J. Am. Chem. Soc.*, 1992, **114**, 10583.
4 P. D. Beer, Z. Chen, M. G. B. Drew, J. Kingston, M. Ogden and P. Spencer, *J. Chem. Soc., Chem. Commun.*, 1993, 1046.
5 A. Benito, J. Cano, R. Martínez-Máñez, J. Soto, J. Payá, F. Lloret, M. Julve, J. Faus and M. D. Marcos, *Inorg. Chem.*, 1993, **32**, 1197.
6 G. De Santis, L. Fabbizzi, M. Licchelli and P. Pallavicini, *Inorg. Chim. Acta*, 1994, **225**, 239.
7 M. J. L. Tendero, A. Benito, J. Cano, J. M. Lloris, R. Martínez-Máñez, J. Soto, A. J. Edwards, P. R. Raithby and M. A. Rennie, *J. Chem. Soc., Chem. Commun.*, 1995, 1643.
8 A. Ori and S. Shinkai, *J. Chem. Soc., Chem. Commun.*, 1995, 1771.
9 C. Dusemund, K. R. A. S. Sandanayake and S. Shinkai, *J. Chem. Soc., Chem. Commun.*, 1995, 333.

10 M. J. L. Tendero, A. Benito, R. Martínez-Máñez, J. Soto, J. Payá, A. J. Edwards and P. R. Raithby, *J. Chem. Soc.*, *Dalton Trans.*, 1996, 343.
11 M. J. L. Tendero, A. Benito, R. Matínez-Máñez, J. Soto, E. García-España, J. A. Ramírez, M. I. Burguete and S. V. Luis, *J. Chem. Soc.*, *Dalton Trans.*, 1996, 2923.
12 M. J. L. Tendero, A. Benito, R. Martínez-Máñez and J. Soto, *J. Chem. Soc.*, *Dalton Trans.*, 1996, 4121.
13 P. D. Beer, Z. Chen, M. G. B. Drew, A. O. M. Johnson, D. K. Smith and P. Spencer, *Inorg. Chim. Acta*, 1996, **246**, 143.
14 H. Yamamoto, A. Ori, K. Ueda, C. Dusemund and S. Shinkai, *Chem. Commun.*, 1996, 407.
15 R. C. Mucic, M. K. Herrlein, C. A. Mirkin and R. L. Letsinger, *Chem. Commun.*, 1996, 555.
16 A. Benito, R. Martínez-Máñez, J. Soto and M. J. L. Tendero, *J. Chem. Soc.*, *Faraday Trans.*, 1997, 2175.
17 M. E. Padilla-Tosta, R. Martínez-Máñez, T. Pardo, J. Soto and M. J. L. Tendero, *Chem. Commun.*, 1997, 887.
18 P. D. Beer, M. G. B. Drew and D. K. Smith, *J. Organomet. Chem.*, 1997, **543**, 259.
19 H. Plenio, D. Burth and R. Vogler, *Chem. Ber.*, 1997, **130**, 1405.
20 A. Benito, J. M. Lloris, R. Martínez-Máñez and J. Soto, *Polyhedron*, 1998, **17**, 491.
21 J. M. Lloris, R. Martínez-Máñez, T. Pardo, J. Soto and M. E. Padilla-Tosta, *Chem. Commun.*, 1998, 837.
22 J. M. Lloris, R. Martínez-Máñez, T. Pardo, J. Soto and M. E. Padilla-Tosta, *J. Chem. Soc.*, *Dalton Trans.*, 1998, 2635.
23 J. M. Lloris, R. Martínez-Máñez, M. E. Padilla-Tosta, T. Pardo, J. Soto and M. J. L. Tendero, *J. Chem. Soc.*, *Dalton Trans.*, 1998, 3657.
24 J. M. Lloris, A. Benito, R. Martínez-Máñez, M. E. Padilla-Tosta, T. Pardo, J. Soto and M. J. L. Tendero, *Helv. Chim. Acta*, 1998, **81**, 2024.
25 P. D. Beer, J. Cadman, J. M. Lloris, R. Martínez-Máñez, M. E. Padilla-Tosta, T. Pardo, D. K. Smith and J. Soto, *J. Chem. Soc.*, *Dalton Trans.*, 1999, 127.
26 G. Gran, *Analyst* (*London*), 1952, **77**, 661; F. J. Rossotti and H. J. Rossotti, *J. Chem. Educ.*, 1965, **42**, 375.
27 P. Gans, A. Sabatini and A. Vacca, *J. Chem. Soc.*, *Dalton, Trans.*, 1985, 1195.
28 P. D. Beer and D. K. Smith, *J. Chem. Soc.*, *Dalton Trans.*, 1998, 417.
29 SHELXTL, Version 5.03, Siemens Analytical X-Ray Instruments, Madison, WI, 1994.
30 J. Cano, A. Benito, R. Martínez-Máñez, J. Soto, J. Payá, F. Lloret, M. Julve, M. D. Marcos and E. Sinn, *Inorg. Chim. Acta*, 1995, **231**, 45.
31 E. Luboch, A. Cygan and J. F. Biernat, *Inorg. Chim. Acta*, 1983, **68**, 201.
32 K. A. Byriel, K. R. Dunster, L. R. Gahan, C. H. L. Kennard, J. L. Latten and I. L. Swann, *Inorg. Chim. Acta*, 1993, **205**, 191.

Paper 9/02008J